A continuous point measure for quantifying skull deformation in medical diagnostics

Herbert F. Jelinek[1,2,3], *Ben Strachan*[3], *Bridget O'Connor*[4], *Ahsan Khandoker*[2]

[1]*Australian School of Advanced Medicine, Macquarie University, Sydney, Australia*
[2]*Department of Biomedical Engineering, Khalifa University, Abu Dhabi, United Arab Emirates*
[3]*Centre for Research in Complex Systems and School of Community Health, Charles Sturt University, Albury, Australia*
[4]*Paediatric Physiotherapy Unit, Gateway Community Health Centre, Wodonga, Australia*
E-mail: hjelinek@csu.edu.au

Published in Healthcare Technology Letters; Received on 28th November 2013; Revised on 14th April 2014; Accepted on 14th April 2014

Deformational plagiocephaly (DP) manifests in a deformed skull primarily caused by retaining a constant sleeping position in infants. Manual measures of skull asymmetry based on MRI or CT scans combined with the cranial vault asymmetry index (CVAI) provides information on the extent of asymmetry. CVAI uses four points on the skull as markers for the asymmetry index but tends to underestimate the deformity because of the lack of sampling points. Computer-based continuous-point methods may be a more objective measure with better sensitivity for the skull contour. The outline of the skull circumference of infants with confirmed cranial deformity was obtained from the literature and analysed applying the mean bending energy (MBE) obtained from the Hermitian wavelet. MBE was shown to correlate with CVAI in the current sample and has the potential to add both quantitative and visual information in 2D or 3D space for the clinician to diagnose DP. Wavelet-based continuous-point estimation of skull asymmetry is a useful method as it is more sensitive to mild deformation anywhere along the skull outline and in assessing slow but progressive improvement as a result of treatment. The broader significance is that this method can be applied to other structural pathology analysis in clinical practice.

1. Introduction: Deformational plagiocephaly (DP) is an asymmetric distortion of the skull, most often resulting from external forces such as maintaining a constant sleeping position in early infancy when the skull of the infant is still soft [1].

In clinical practice DP is measured using either precision calipers, MRI, CT scans, visual assessment charts, thermoplastic bands or photography from which a manually derived asymmetry index such as the cranial vault asymmetry index (CVAI) is determined [2]. The CVAI is calculated as indicated in Fig. 1 and explained in section 2. Importantly for PD determination and effectiveness of treatment, the CVAI utilises four points along the skull outline to determine the asymmetry (see (1)) and is therefore prone to error that occurs when only the length of the diagonals across the endocranial surface is measured. As shown in Fig. 1 schematically, the length of the two diagonals is not different between the left- and right-hand side despite the change in the asymmetry.

Being able to automatically quantify the morphology or deformity of the cross-sectional skull outline from thermoplastic bands, CT or MRI images would be a significant advance in PD evaluation. A continuous-point measure is more sensitive in assessing slow but progressive improvement as a result of early non-invasive therapy, such as repositioning the patient by assessing the whole cross-sectional contour of the skull as well as contour changes, which are not in the vicinity of the two diagonals required to obtain the CVAI (Fig. 1). The continuous-point method may also be useful for assessing a wide range of other morphological deformities in clinical practice including craniostenosis and brachycephaly.

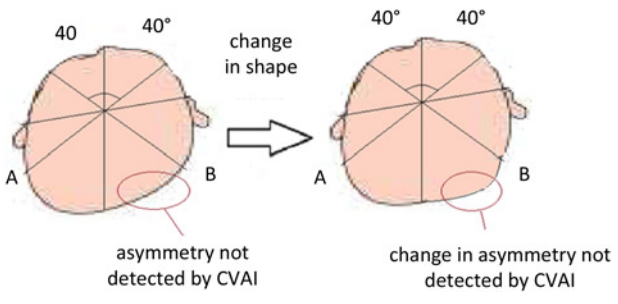

Figure 1 *Inaccuracy associated with use of CVAI method*

Continuous measures such as curvature, mean bending energy (MBE) or area derived from the wavelet transform use all the points on the skull's transverse contour and can be used to classify an infant's transverse skull asymmetry.

The continuous wavelet transform (CWT) has been extensively applied in many different fields such as signal and image processing, astronomy, finance and neuroscience. In particular, wavelets are able to detect singularities, making it a powerful tool for image segmentation [3] and feature extraction [4], as they provide information on the image of interest with respect to the wavelet form [5].

2. Method: The original greyscale images were published MRI representations of clinically confirmed cases of plagiocephaly. The published greyscale MRI cross-sections were thresholded to remove soft tissue and leave the bony structures for evaluation as shown in [6]. The endocranial view of the MRI was determined by the craniofacial surgeon [6]. For determining the CVAI and wavelet derived parameters, the greyscale images from the publication were scanned and converted to binary images, retaining only the outline of each cross-sectional skull image by thresholding.

2.1. Cranial vault asymmetry: The CVAI was calculated as outlined in [7] and the equation given below

$$\mathrm{CVAI} = \frac{abs(A - B)}{\min(A, B)} \tag{1}$$

where A and B are the diagonals (Fig. 1).

Briefly, the CVAI was calculated by dividing the skull circumference as determined by MRI at the level above the ridge of the nose and ears into quadrants with a line connecting the ears and a perpendicular line drawn with the centre of the nose as reference. From the

doi: 10.1049/htl.2013.0029

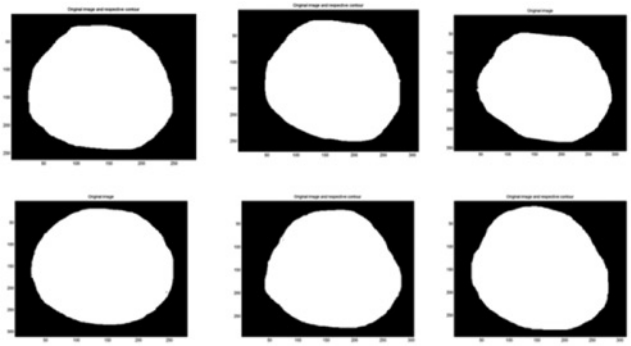

Figure 2 *Skull circumference of MRI pathology images*

intersection of these two lines, 40° is measured to the left and right giving two diagonals (*A* and *B*). The length of the diagonals is measured and the difference in length of the diagonals divided by the smaller diagonal provides the asymmetry index expressed as a percentage (Fig. 2). A value greater than 3.5% regardless of head circumference is defined as significant asymmetry.

2.2. Continuous point measure: From a basic wavelet function, namely, the mother wavelet $\psi(x)$, a set of basis functions may be derived by translation and scaling the wavelet, that is

$$\psi_{a,b}(x) = \frac{1}{\sqrt{a}}\psi\left(\frac{x-b}{a}\right) \tag{2}$$

where a and b are the scale and translation parameters and $1/\sqrt{a}$ is a normalisation constant to preserve the wavelet energy throughout scales. The CWT itself may be defined as in [8]

$$T_{\psi}[f](b,a) = \langle f, \psi_{a,b}\rangle = \int_{-\infty}^{\infty} f(x,y)\psi_{a,b}(x,y)\mathrm{d}x\mathrm{d}y \tag{3}$$

where in the context of this work, $f(x, y)$ is the image to be analysed.

Here we utilise the gradient of the Gaussian function to compose the first Hermitian wavelet in 2D

$$\psi_g(x,y) = \nabla g(x,y) = \hat{i}\,\frac{\partial_g(x,y)}{\partial x} + \hat{j}\,\frac{\partial_g(x,y)}{\partial y} \tag{4}$$

where $\psi_{1(x,\,y)}$ and $\psi_{2(x,\,y)}$ are the directional components defined as partial derivatives of the Gaussian $g(x, y)$, that is

$$\psi_{1(x,y)} = \frac{\partial g(x,y)}{\partial x} \text{ and } \psi_{2(x,y)} = \frac{\partial g(x,y)}{\partial y}$$

where $g(x, y)$ denotes the circularly symmetric 2D Gaussian [5], whose standard deviation plays the role of the wavelet scale parameter. By using $\psi_{1(x,\,y)}$ and $\psi_{2(x,\,y)}$ as wavelets, the first Hermitian wavelet in 2D is calculated by

$$[f](a,b) = \begin{pmatrix} T_{\psi 1}[f](b,a) \\ T_{\psi 2}[f](b,a) \end{pmatrix} \tag{5}$$

where ψ, f, b and a denote the analysing wavelet, the analysed image, the displacement vector and the scale parameter, respectively. The wavelet transform

$$T_{\psi}[f](a,b) \tag{6}$$

for each pair (b, a) is a vector whose components are coefficients of the wavelet transform using $\psi_{1(x,\,y)}$ and $\psi_{2(x,\,y)}$ as the analysing wavelets. Taking advantage of the convolution theorem, the wavelet transform was implemented and calculated in the Fourier domain, yielding a time complexity of

$$\Theta\left(N \log_2 N\right) \tag{7}$$

The scale parameter a in this work was chosen manually at 10–6 in the Fourier domain. The curvature can then be calculated based on the wavelet transform components shown in the next section. The MBE may then be derived from the curvature.

2.2.1 Mean bending energy: Taking the skeleton outline of the skull circumference as the trajectory trace from a moving punctual particle, the trajectory curvature $k(x, y)$ represents how the direction of a unit tangent vector varies along the shape contour $c(x, y)$, c standing for the curvature function $c(x, y)$, being defined by

$$k = \nabla.\frac{\nabla c}{\|\nabla c\|} = \frac{c_{xx}c_y^2 - 2c_xc_yc_{xy} + c_{yy}c_x^2}{\left(c_x^2 - c_y^2\right)^{(3/2)}} \tag{8}$$

where c_x, c_y, c_{xx}, c_{yy} and c_{xy} denote the first partial derivatives of c with respect to x and y, the second partial derivatives of c with respect to x and y and the partial derivative with respect to x and y [9]. The 2D wavelet transform components are used to estimate these partial derivatives.

The MBE is a curvature-based shape descriptor, whose discretised version is defined as [10]

$$\hat{B} = \frac{1}{N}\sum_{n=0}^{N-1} k(n)^2 \tag{9}$$

where N is the number of pixels in the contour and $k(n)$ is the local curvature for the nth pixel in the contour.

3. Results: The images used for analysis display various grades of skull deformation (Fig. 2). MBE increases with CVAI in these selected images. The results shown in Table 1 indicate that for these selected images MBE is correlated with CVAI.

4. Discussion: Our results for the current images indicate that MBE correlates with the CVAI measures in magnitude and therefore has the potential to be used in clinical practice. The advantage of using MBE is that it is not dependent on identifying the location of the nose and ears for calculations nor the necessity to accurately determine the 40° intersections and length measurements for correct calculation of the reference diameters and determining skull asymmetry. In addition, MBE provides a global feature and is thus more sensitive to changes in skull deformity anywhere along the perimeter.

Clinically, the location of skull asymmetry can vary outside the zone identified with the 40° markers. In this case, CVAI will not

Table 1 CVAI and bending energy for six images with skull deformity

Image	CVAI	MBE ($\times 10^{-2}$)
1	3.1	5.26
2	3.3	5.5
3	7.14	5.61
4	12.12	6.94
5	15.63	8.28
6	20.68	8.87

accurately assess asymmetry and will differ from the result obtained by MBE.

The MBE is proportional to the amount of energy required to change the shape of interest to the lowest energy shape, a perfect circle [11]. The skull is an oblong/elliptical shape that becomes deformed to a different extent depending on pathology. Any flattening or bulging of the skull because of a deformity requires a different amount of energy, which is represented by the magnitude of the MBE. In clinical practice it is important to identify local deformities including deformities that fall outside the 40° zone within which CVAI is most sensitive, prior and following therapy. These changes outside the 40° zone are expected to be missed depending on the placement of the diagonal lines for CVAI calculation with respect to the anomaly. Hence valuable assessment information indicating skull deformity and effect of treatment is lost.

Future work will concentrate on obtaining control images to establish a normal range using MBE and also using thermoplastic bands for calculation of the CVAI to compare to MBE results in cases where CVAI is unable to identify a change in asymmetry following therapy.

5. Conclusion: Clinical implications of this work represent the use of a wavelet transform imaging analysis tool to improve clinical decision making by providing a robust measure of skull circumference deformity and the effect of treatment, which includes all points on the cross-sectional contour of the skull. The method can be used in a variety of applications in addition to skull contour, where X-ray, MRI or CT images represent outlines of bones, organs, tumours or circulation.

6. Acknowledgments: The authors wish to thank Jorge G.J. Leandro and Roberto M. Cesar Jr. for providing the Matlab scripts, and Hanin Abubaker for technical assistance.

7 References

[1] Bialocerkowski A., Vladusic S., Ng C.: 'Prevalence, risk factors, and natural history of positional plagiocephaly: a systematic review', *Dev. Med. Child Neurol.*, 2008, **50**, (8), pp. 577–586

[2] Captier G., Leboucq N., Bigorre M., *ET AL.*: 'Plagiocephaly: morphometry of skull base asymmetry', *Surg. Radiol. Anat.*, 2003, **25**, pp. 226–233

[3] Cesar R.M. Jr., Jelinek H.F.: 'Segmentation of retinal fundus vasculature in nonmydriatic camera images using wavelets', in Suri J.S., Laxminarayan S. (Eds.): 'Angiography and plaque imaging' (CRC Press, London, 2003), pp. 193–224

[4] Jelinek H.F., Cesar R.M. Jr., Leandro J.J.G.: 'Exploring wavelet transforms for morphological differentiation between functionally different cat retinal ganglion cells', *Brain Mind*, 2003, **4**, pp. 67–90

[5] Arnéodo A., Decoster N., Roux S.G.: 'A wavelet-based method for multifractal image analysis: I. Methodology and test applications on isotropic and anisotropic random rough surfaces', *Eur. Phys. J. B*, 2000, **15**, pp. 567–600

[6] Yu C.-C., Wong F.-W., Lo L.-J., Chen Y.-R.: 'Craniofacial deformity in patients with uncorrected congenital muscular torticollis: an assessment from three-dimensional computed tomography imaging', *Plast. Reconstr. Surg.*, 2004, **113**, (1), pp. 24–33

[7] Loveday B., De Chalain T.B.: 'Active counterpositioning or orthotic device to treat positional plagiocephaly?', *J. Craniofacial Surg.*, 2001, **12**, (4), pp. 308–313

[8] Castleman K.R.: 'Digital image processing' (Prentice-Hall, London, 1995)

[9] Estrozi L.F., Rios L.G., Campos A.G., Cesar R.M. Jr., Costa L.da F.: '1D and 2D Fourier-based approaches to numeric curvature estimation and their comparative performance assessment', *Digit. Signal Process.*, 2003, **13**, pp. 172–197

[10] Costa L.da F., Cesar R.M. Jr.: 'Shape analysis and classification: theory and practice' (CRC Press, 2001)

[11] Cesar R.M. Jr., Costa L. da F.: 'Shape characterization in natural scales by using the multiscale bending energy'. Proc. 13th ICPR – Int. Conf. on Pattern Recognition 1996, Technical University of Vienna, Austria, 1996, pp. 735–739

doi: 10.1049/htl.2013.0029